ELECTRONIC SUPPLEMENTARY INFORMATION

Fluorescent surface-grafted block copolymer brushes obtained in a versatile post-polymerization approach

Piotr Wieczorek,[a,b] Tomasz Kuciel,[a] Tomasz Uchacz,[a*] Szczepan Zapotoczny[a*]

[a] *Jagiellonian University, Faculty of Chemistry, Gronostajowa 2, 30-387, Krakow, Poland*

[b] *Doctoral School of Exact and Natural Sciences, Jagiellonian University, Lojasiewicza 11, 30-348 Krakow, Poland*

[*] Corresponding author: tomasz.uchacz@uj.edu.pl (TU), s.zapotoczny@uj.edu.pl (SZ)

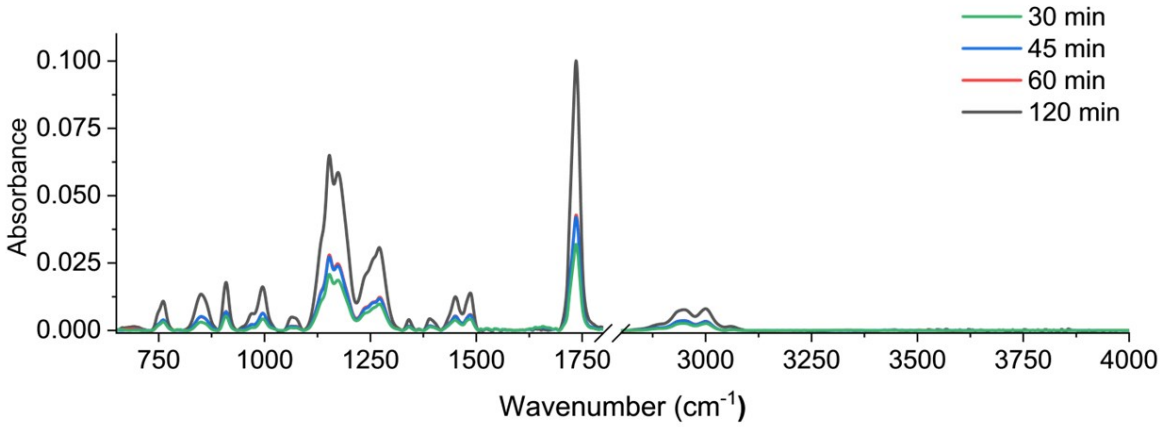

Figure S1. FTIR spectra of poly(GMA) brushes obtained after various polymerization times.

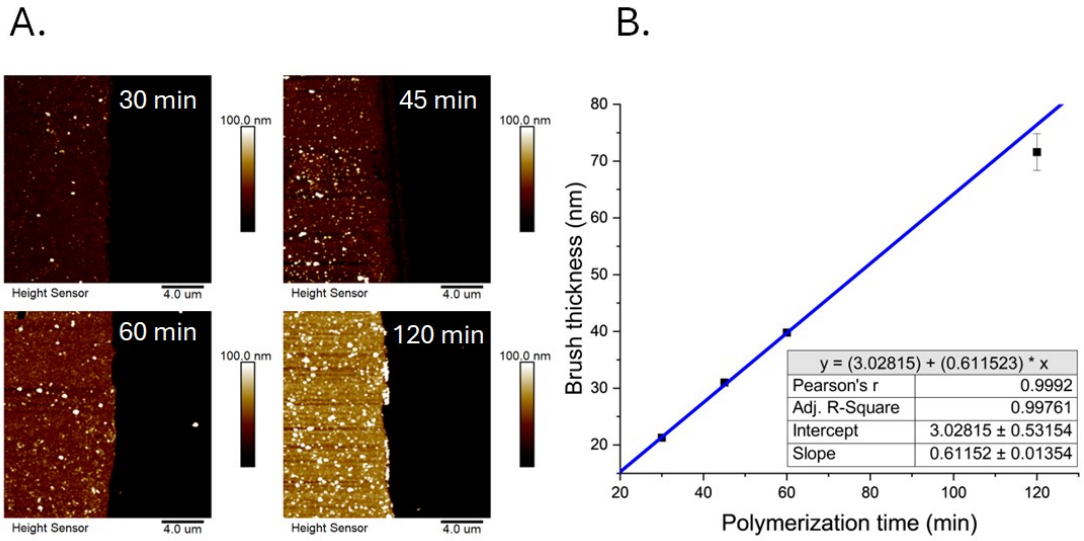

Figure S2. (A) AFM topography images in air of mechanically made scratches of poly(GMA) brushes after various polymerization time, and (B) dependence of the polymer brush thickness determined from those AFM images on polymerization time fitted to a line using linear regression.

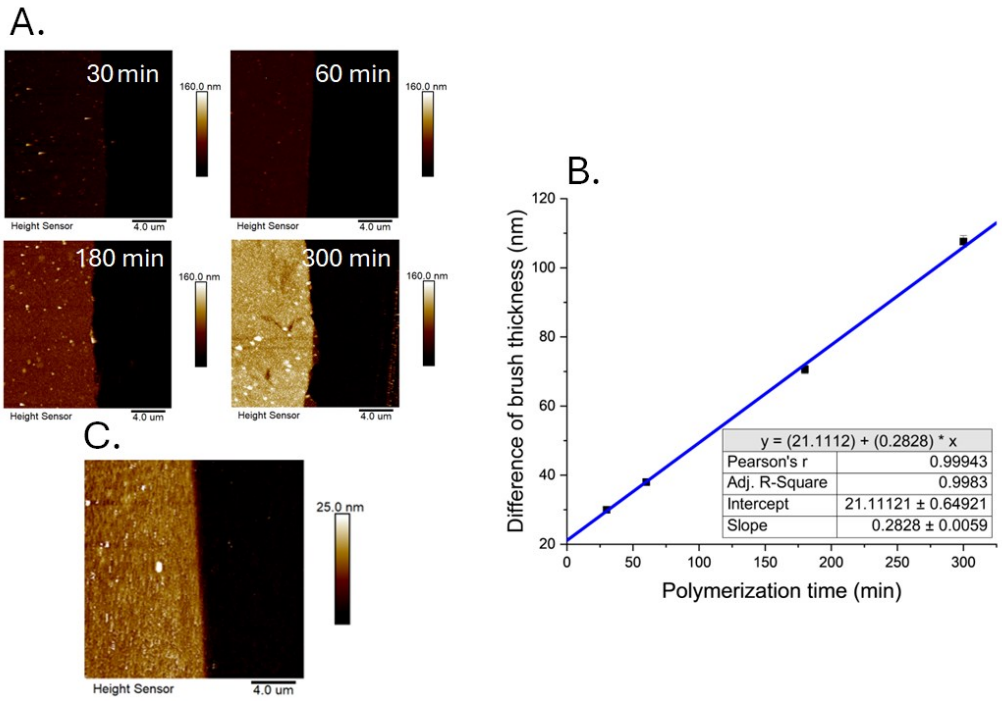

Figure S3. AFM topography images in air of mechanically made scratches of (A) poly(GMA) brushes after extensions of the chains of the native brush presented in (C) after various polymerization times; (B) dependence of the polymer brush thickness difference determined from those AFM images on polymerization time fitted to a line using linear regression.

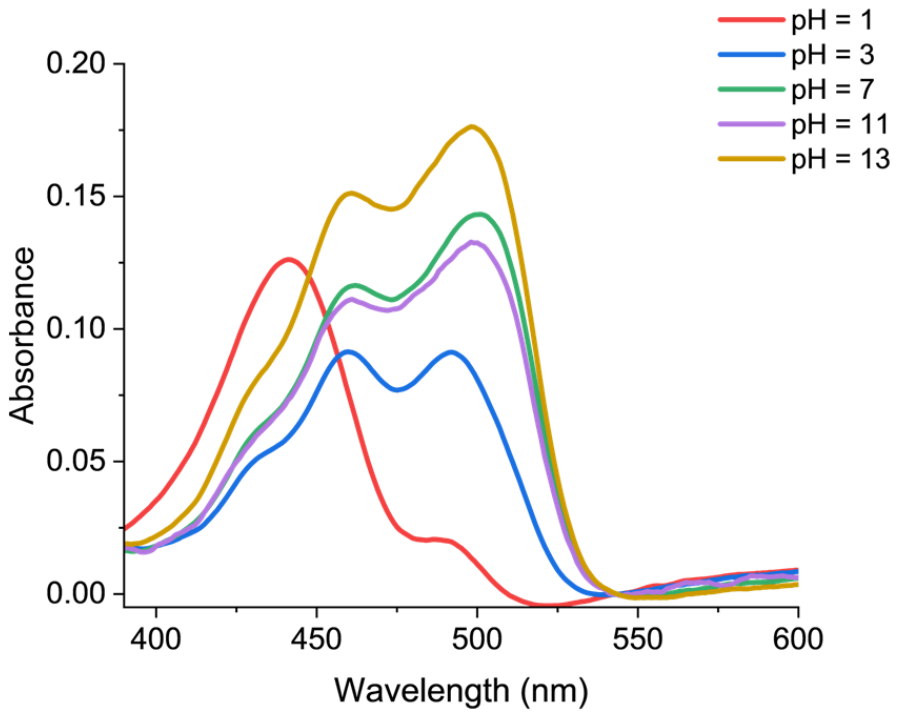

Figure S4. UV-Vis absorption spectra of poly(GMA[6AF]) (N1) brushes measured in aqueous solutions of various pH.

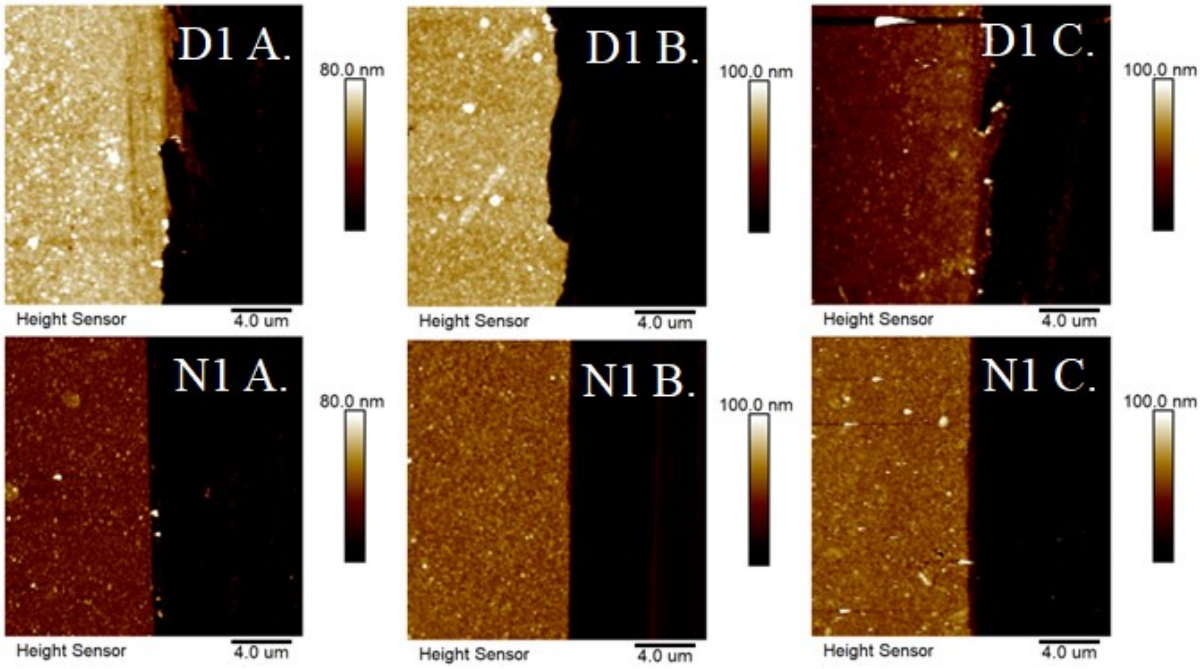

Figure S5. AFM topography images in air of D1 and N1 brushes after various stages of modification: (A) native poly(GMA), (B) poly(GMA[6AF]) and (C) poly(GMA[6AF]-block-GMA).

Table S1. Thickness changes of polymer brushes (N1 and D1 samples) after post-polymerization modifications.

Polymer brush	Native brush thickness (nm)	Brush thickness after reaction with 6AF (nm)	Brush thickness after chain-extension reaction (nm)
N1	32.6 ± 0.3	54.7 ± 0.8	55.8 ± 1.2
D1	62.9 ± 0.4	72.7 ± 0.7	-

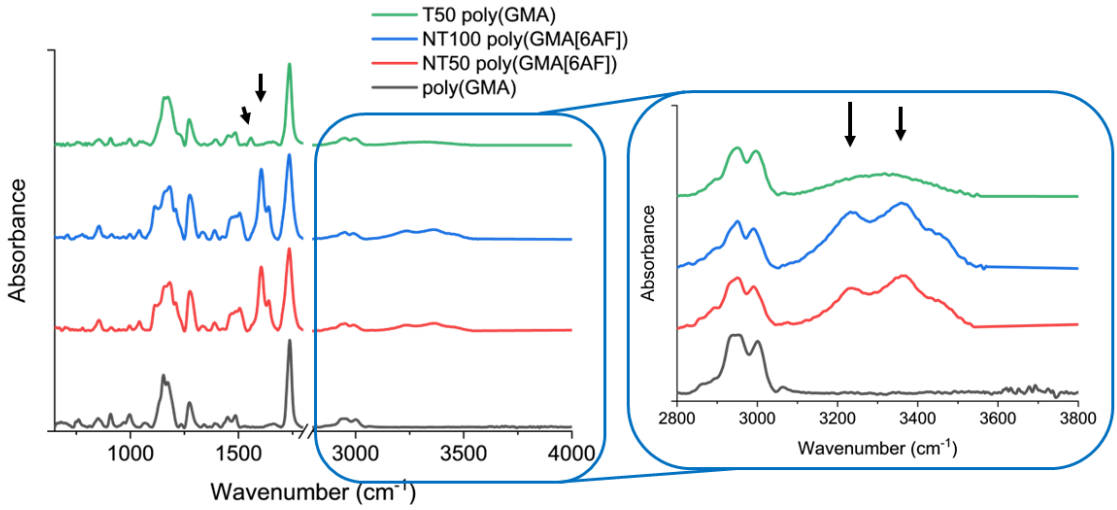

Figure S6. Comparison of the FTIR spectra of T50, NT50, NT100 and poly(GMA) brushes with zoomed part in on the 2800-3800 cm^{-1} range.

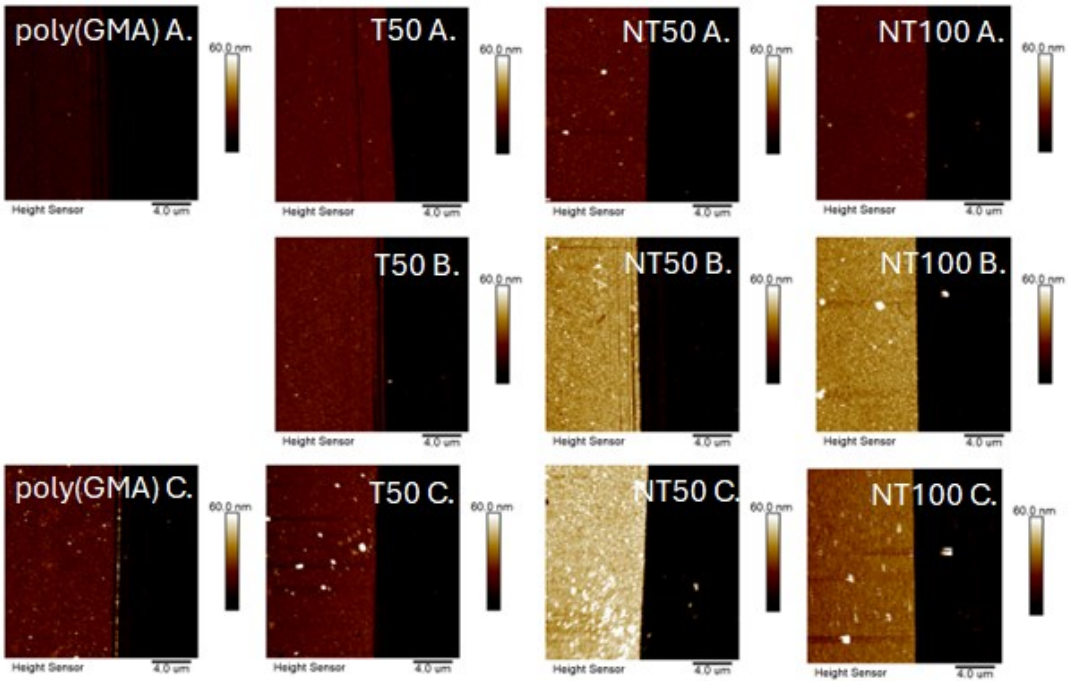

Figure S7. AFM topography images in air of poly(GMA) brushes (R1, T50, NT50 and NT100) with different stages of modification: (A) poly(GMA), (B) after treatment in $MeNO_2$ and (C) after chain extension.

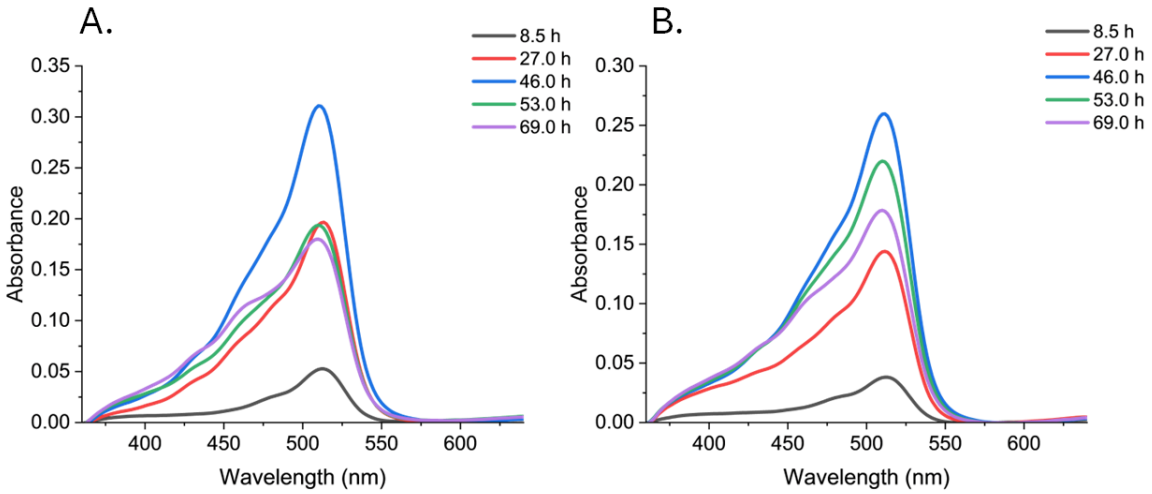

Figure S8. UV-Vis spectra of dry poly(GMA[6AF]) (A) NT50 and (B) NT100 brushes measured after various times of the reaction with 6AF.

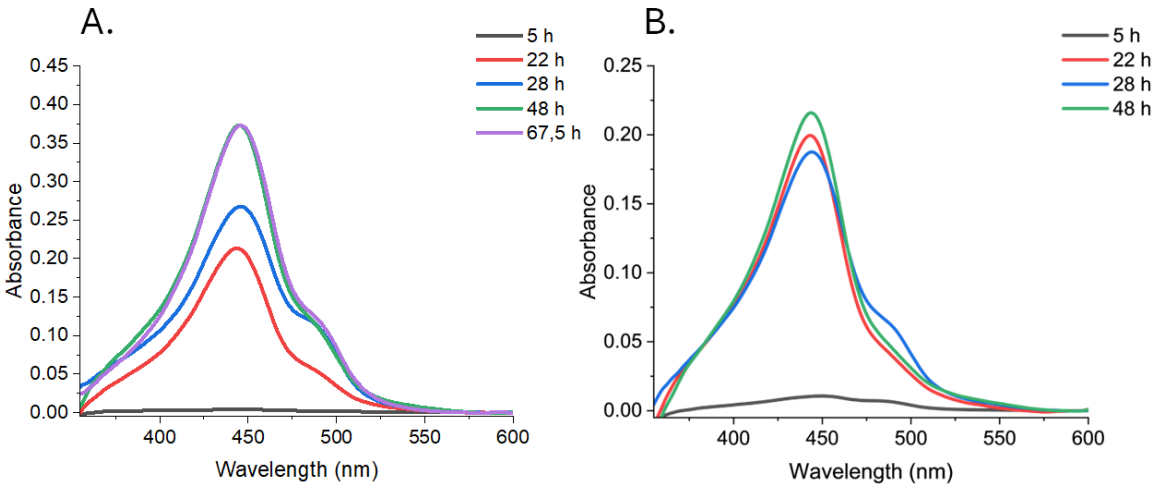

Figure S9. UV-Vis spectra of (A) NP5 and (B) NP20 polymer brushes measured in $MeNO_2$ after various times of the reaction with 6AF.

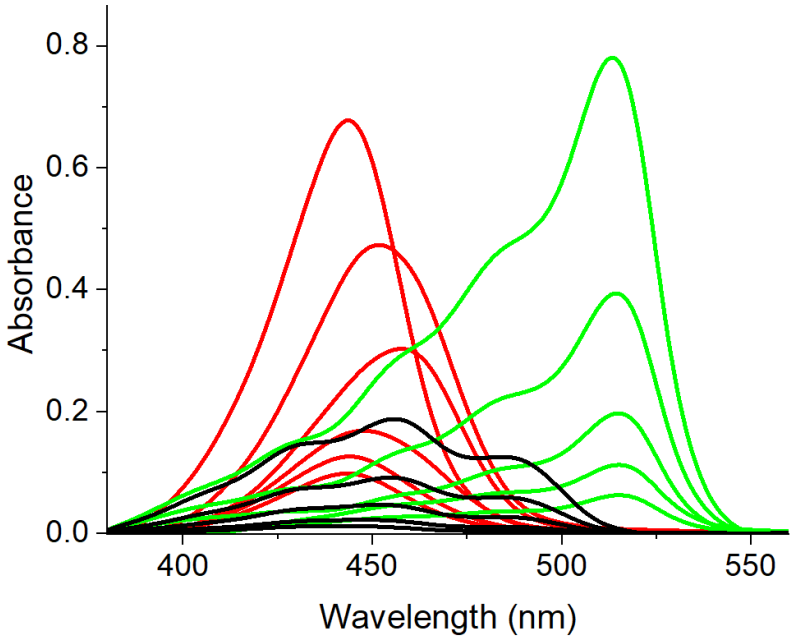

Figure S10. UV-Vis absorption spectra of 6AF in: $MeNO_2$ (black; c_{6AF} = 0.08 - 1.25 mM), 5 µl/ml PMDETA in $MeNO_2$ (green; c_{6AF} = 0.01 - 0.16 mM), 0.5 mM HCl in $MeNO_2$ (red; c_{6AF} = 0.01 - 0.16 mM).

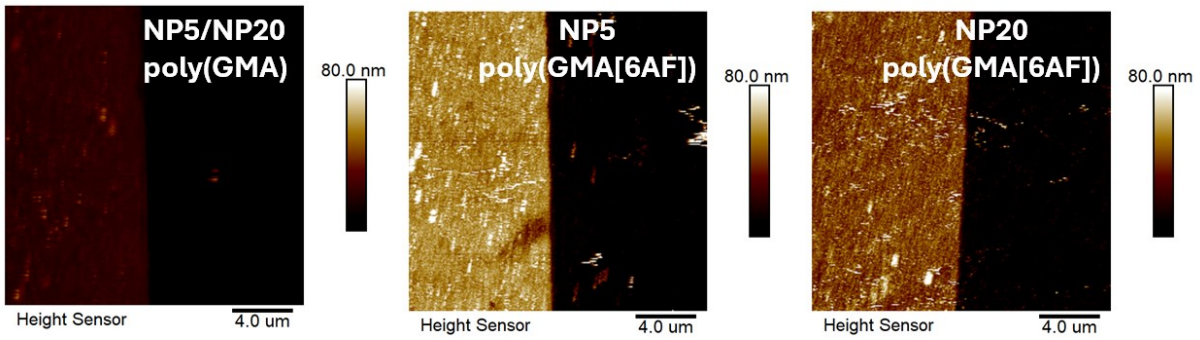

Figure S11. AFM topography images in air of NP5/NP20 poly(GMA), NP5 poly(GMA[6AF]) and NP20 poly(GMA[6AF]).

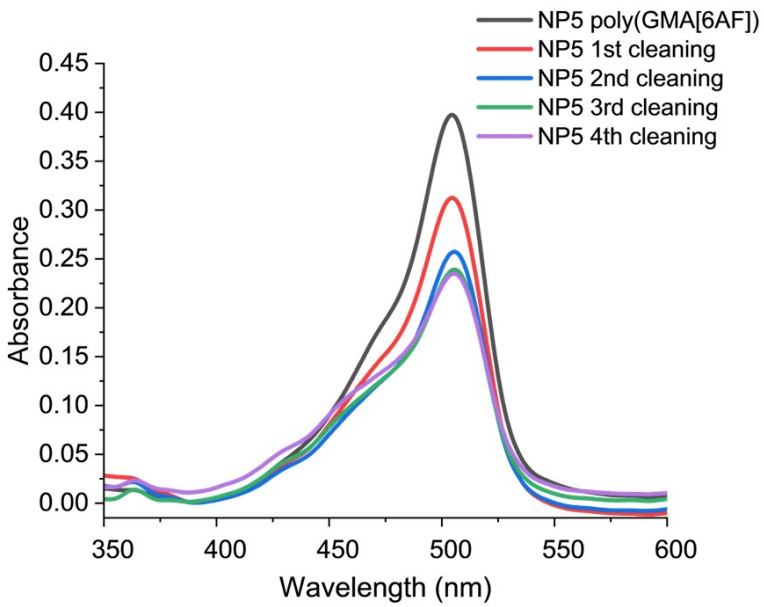

Figure S12. UV-Vis spectra in MeOH of NP5 brush after successive cleaning cycles.

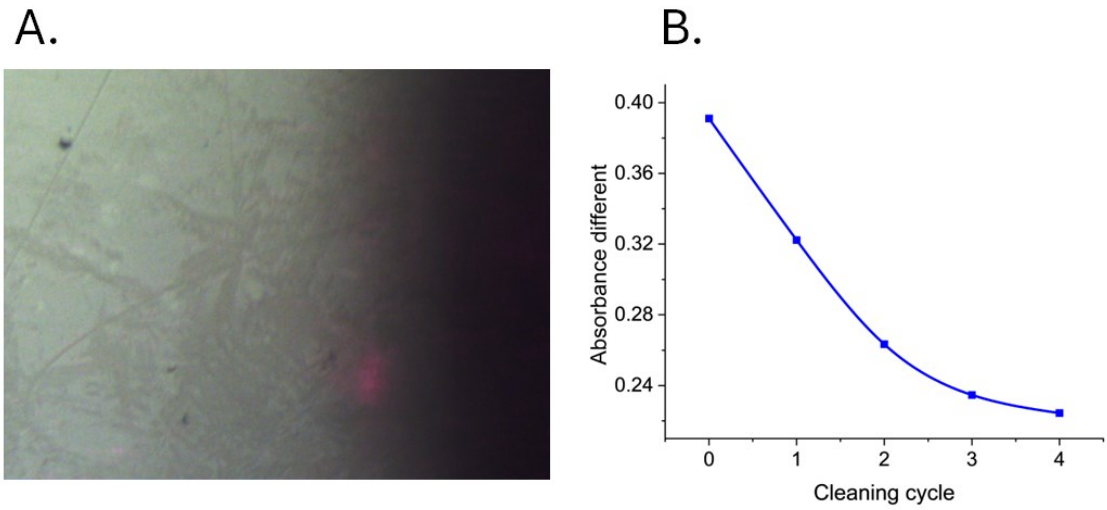

Figure S13. (A) An optical microscope (in AFM instrument) image of NP5 brush after cleaning, (B) absorbance difference from UV-Vis spectra in MeOH of the NP5 brush between the value at 510 nm (maximum) and 600 nm (baseline) shown as a function of the number of cleaning cycles.

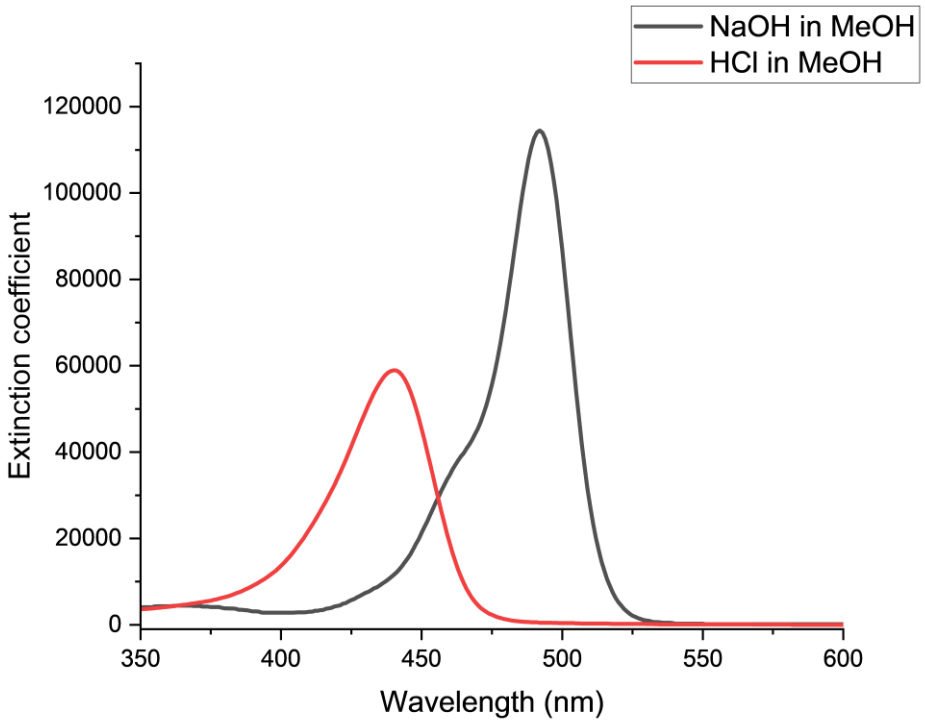

Figure S14. UV-Vis spectra of 6AF in MeOH: alkaline solution (black; 0.1 mM NaOH), acid solution (red; 0.1 M HCl).

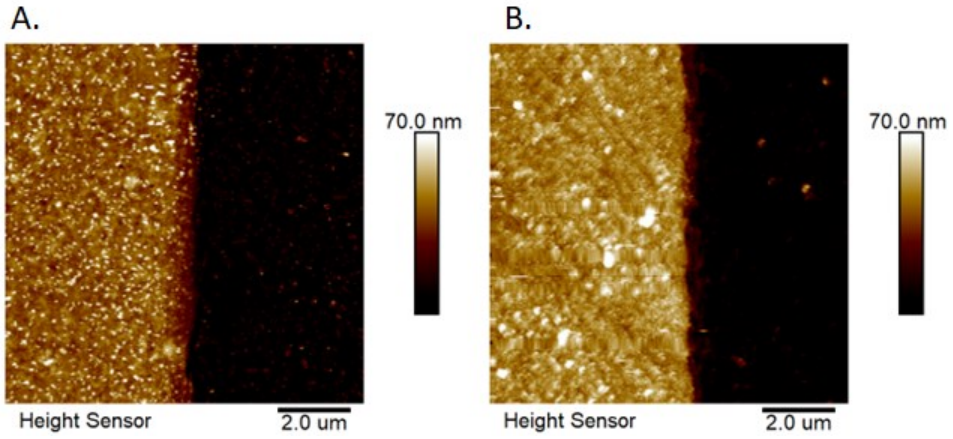

Figure S15. AFM topography images (A) in air and (B) in MeOH of poly(GMA[6AF]) brushes.